ACCOUNTS of chemical research

Article

pubs.acs.org/accounts

Modeling Photoionization of Aqueous DNA and Its Components

Eva Pluhařová,[†,§] Petr Slavíček,*[,‡] and Pavel Jungwirth*[,†]

[†]Institute of Organic Chemistry and Biochemistry, Academy of Sciences of the Czech Republic, Flemingovo nám. 2, 16610 Prague 6, Czech Republic

[‡]University of Chemistry and Technology, Department of Physical Chemistry, Technická 5, 16628 Prague 6, Czech Republic

CONSPECTUS: Radiation damage to DNA is usually considered in terms of UVA and UVB radiation. These ultraviolet rays, which are part of the solar spectrum, can indeed cause chemical lesions in DNA, triggered by photoexcitation particularly in the UVB range. Damage can, however, be also caused by higher energy radiation, which can ionize directly the DNA or its immediate surroundings, leading to indirect damage. Thanks to absorption in the atmosphere, the intensity of such ionizing radiation is negligible in the solar spectrum at the surface of Earth. Nevertheless, such an ionizing scenario can become dangerously plausible for astronauts or flight personnel, as well as for persons present at nuclear power plant accidents. On the beneficial side, ionizing radiation is employed as means for destroying the DNA of cancer cells during radiation therapy.

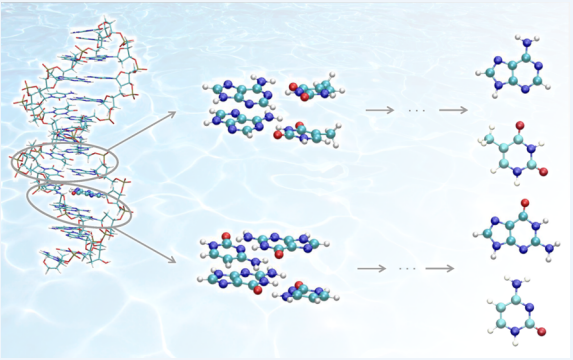

Quantitative information about ionization of DNA and its components is important not only for DNA radiation damage, but also for understanding redox properties of DNA in redox sensing or labeling, as well as charge migration along the double helix in nanoelectronics applications. Until recently, the vast majority of experimental and computational data on DNA ionization was pertinent to its components in the gas phase, which is far from its native aqueous environment. The situation has, however, changed for the better due to the advent of photoelectron spectroscopy in liquid microjets and its most recent application to photoionization of aqueous nucleosides, nucleotides, and larger DNA fragments.

Here, we present a consistent and efficient computational methodology, which allows to accurately evaluate ionization energies and model photoelectron spectra of aqueous DNA and its individual components. After careful benchmarking, the method based on density functional theory and its time-dependent variant with properly chosen hybrid functionals and polarizable continuum solvent model provides ionization energies with accuracy of 0.2−0.3 eV, allowing for faithful modeling and interpretation of DNA photoionization. The key finding is that the aqueous medium is remarkably efficient in screening the interactions within DNA such that, unlike in the gas phase, ionization of a base, nucleoside, or nucleotide depends only very weakly on the particular DNA context. An exception is the electronic interaction between neighboring bases which can lead to sequence-specific effects, such as a partial delocalization of the cationic hole upon ionization enabled by presence of adjacent bases of the same type.

1. INTRODUCTION

Nucleic acids are oxidized by reactive oxygen species (ROS) or directly by high-energy radiation. Formation and mobility of a cationic hole in nucleic acids attract attention due to several reasons. First, oxidation of nucleic acids causes serious structural defects of genomic DNA, for example, single and double strand breaks.[1] These changes may lead to mutations and ultimately to cancer.[2] Next, mobility of a cationic hole plays also an important role in redox sensing and redox labeling.[3] Charge transfer along DNA strands also forms the mechanistic basis for nucleic acid based nanoelectronics.[4] Indeed, ionized DNA represents a remarkable material. It has been found, for instance, that charge can migrate along the double helix to distances as large as 200 Å.[3,5] Charge is ultimately trapped in sites with low ionization energy; guanine bases typically serve for this purpose.[6,7]

DNA is a complex electrochemical system as hundreds of redox sites need to be considered at once. The essential step that can clarify DNA oxidation at a molecular level is to describe basic physicochemical characteristics of DNA components in their native environment. These encompass ionization energies, reorganization energies, redox potentials, and equilibrium constants of protolytic reactions both in the neutral and ionized state.[8−10] Let us assume an example of cationic hole transfer in a nucleic acid. The rate constants of charge transfer can be calculated within the Marcus theory, provided that we know the potential of the driving force of charge transfer ΔG, the electronic coupling between a donor and acceptor V_{12}, and the reorganization energy λ.[5,11] These quantities are estimated from the ionization energies of donor and acceptor moieties in their native environment.[11]

There has been an enormous effort to characterize the above quantities theoretically and experimentally. In either case, the investigation of the DNA oxidation faces serious conceptual problems. As the computational requirements increase

Received: October 3, 2014
Published: March 4, 2015

DOI: 10.1021/ar500366z
Acc. Chem. Res. 2015, 48, 1209−1217

(typically nonlinearly) with the system size, theory attempts to follow the reductionist path, that is, understand the redox sites in DNA based on calculations on isolated DNA fragments, that is, bases, nucleosides, and nucleotides. Such an approach cannot be accepted without reservation. The properties of the redox sites may be sensitively controlled by isomerism, conformation, hydration, specific interaction between DNA subunits, or presence of counterions.[12,13] These various effects can be at the same time nonadditive. It is thus in no way guaranteed that calculations will converge fast upon increasing model size toward DNA. Experimentally, the oxidation of nucleic acid components has been straightforwardly studied by photoelectron (PE) spectroscopy.[14−22] However, here again the gas phase and cluster systems are not directly linked to the real DNA in its native environment. Ionization parameters of solvated nucleic acid fragments could be estimated only indirectly.[23] The newly emerged liquid microjet technique[24,25] allowed for the first time to directly access ionization energies in hydrated systems, with sufficient system solubility being the only major technical hurdle. Ionization energies of aqueous nucleotides, nucleosides, and larger DNA fragments have been recently estimated by PE experiment and quantum chemical calculations and interpreted with the use of theory.[26,27]

In this Account, we focus on computational modeling of ionization of hydrated DNA within a bottom-up approach. Our work in this field was aimed at interpreting the PE spectroscopy experiments of DNA and its fragments in liquid microjets.[13,26,27] To this end, a fast, yet reliable approach allowing for screening large number of structures was needed. We argue that calculations based on simple dielectric based solvent models combined with properly selected hybrid density functional theory (DFT) functionals represent practical computational counterparts, as well as interpretative tools, for the state-of-the-art PE experiments. We particularly emphasize the role of nuclear and electronic solvation polarization effects which extend beyond the immediate solvent shell around the solute. Based on calculations of realistic DNA fragments, we formulate the minimal model one can use to mimic properties of redox sites in DNA, providing a detailed molecular picture of the primary events of direct radiation damage and redox processes in DNA in its native aqueous environment.

2. IONIZATION ENERGIES: VERTICAL VERSUS ADIABATIC

We aim at accurate, yet efficient, modeling of ionization energies (IEs) of *hydrated* nucleic acid components and nucleic acid fragments using methods of molecular quantum mechanics accounting for solvent effects. The vertical ionization energy (VIE) is defined as the energy difference between an ionized and parent molecule at the geometry of the parent molecule, while for the adiabatic ionization energy (AIE) the geometry of the ionized species is relaxed; see Figure 1. Experimentally, VIE is directly obtained from PE spectroscopy, while AIE can be estimated from the onset of a PE spectrum, providing that the vibrational wave functions of the parent and ionized molecules overlap sufficiently. AIE is also equal to the free energy change connected with the corresponding oxidation reaction and as such it is related to the absolute redox potential of the redox pair. The difference between VIE and AIE is called the relaxation energy λ (Figure 1), which is another important quantity in the theory of charge transfer reactions.

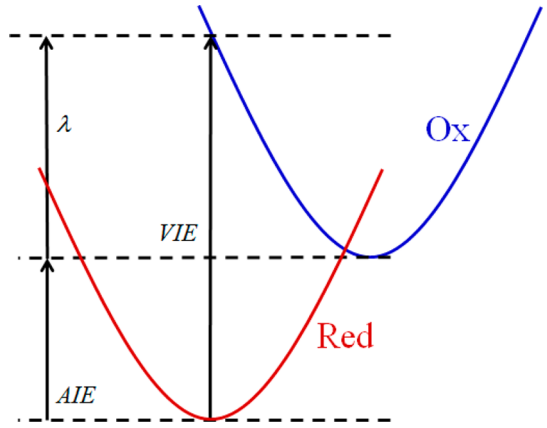

Figure 1. Vertical (VIE) and adiabatic (AIE) ionization energy and their difference, that is, the reorganization energy λ. The energy curves are plotted along a generalized solvent coordinate. Red stands for the reduced state before ionization, while Ox stands for the oxidized state after ionization.

3. CALCULATING IONIZATION ENERGIES: IS DFT GOOD ENOUGH?

Nucleic acid components in solution are rather extended systems with complex interactions. DFT represents a computationally efficient approach allowing for direct investigation of systems with hundreds to thousands of atoms.[28] At the same time, its accuracy needs to be validated. Let us compare here the DFT approaches with computationally more demanding alternatives.

The lowest ionization energy (corresponding to ionization from the HOMO orbital) is calculated as a difference between the ground state energy of the ionized species and that of the parent species, typically using the unrestricted formalism. DFT generally exhibits lower spin contamination compared with wave function based methods and is, therefore, typically applicable for description of ionized states.[28] While the spin contamination can be projected out, for example, in the HF and MP2 calculations,[27] the spin projection is reliable only for systems with small spin contaminations.[29] At the same time, DFT contains the self-interaction error which causes problems for open shell systems and potentially results in artificial charge delocalization between molecular units.[11] It turns out that the cationic hole formed upon ionization is to a large degree localized even for DNA strands composed solely of guanine units. Local and semilocal DFT functionals fail to predict the charge localization. The artificial charge delocalization is, however, to a large extent fixed by using hybrid functionals with a high content of exact exchange.[30]

Calculated IEs sensitively depend on basis set, especially for anionic precursors.[31] The differences for neutral precursors are typically much smaller as can be seen for the results for isolated nucleic acid bases in Table 1. The basis set dependence of the IEs is further reduced upon adding the solvent (for uracil, we performed BMK calculations for up to the aug-cc-pVQZ basis and the VIE is converged with respect to basis set to 0.03 eV). Table 1 also demonstrates that basis set saturation is rather fast for DFT methods.

As we see from a comparison with more advanced electronic structure methods in Table 1, the hybrid DFT functionals are well suited for modeling of ionization in DNA systems. Note at this point that the same functionals are not necessarily suitable for modeling the *structure* of the nucleic acid systems, especially

DOI: 10.1021/ar500366z
Acc. Chem. Res. 2015, 48, 1209−1217

Table 1. Two Lowest VIEs of Nucleic Acid Bases in the Gas Phase Calculated with Different Electronic Structure Methods (The Second VIE for the BMK Method Was Evaluated As the Sum of the Lowest VIE and the Lowest Excitation Energy of the Ionized Species at the Geometry before Ionization)

base →	G	A	C	T	U
BMK/6-31+G*	8.08/9.64	8.34/9.32	8.78/9.39	9.09/10.09	9.55/10.19
BMK/aug-cc-pVTZ	8.05/9.64	8.32/9.32	8.79/9.44	9.07/10.13	9.54/10.23
tuned LC functional BNL/6-31+G*[a]	8.16/9.52	8.46/9.33	8.95/9.61	9.12/9.96	9.66/10.22
tuned LC functional BNL/aug-cc-pVTZ[a]	8.14/9.50	8.46/9.31	8.95/9.58	9.14/9.93	9.69/10.20
EOM-IP/6-31+G*	7.91/9.64	8.15/9.20	8.57/9.23	8.95/9.97	9.35/10.07
EOM-IP/cc-pVTZ[b]	8.15/9.86	8.37/9.37	8.78/9.55	9.13/10.13	9.64/10.38
CASPT2[c]	8.09/9.56	8.37/9.05	8.73/9.42	9.07/9.81	9.42/9.83
expt[d]	8.0−8.3/9.90	8.38/9.45	8.89/9.55	9.19/10.14	9.6/10.13

[a]The LC functional was tuned such that the HOMO energy matches the lowest VIE.[34] [b]Taken from ref 35 (except for U). [c]Taken from ref 36. [d]Data taken from compilation in refs 21, 37, and 38.

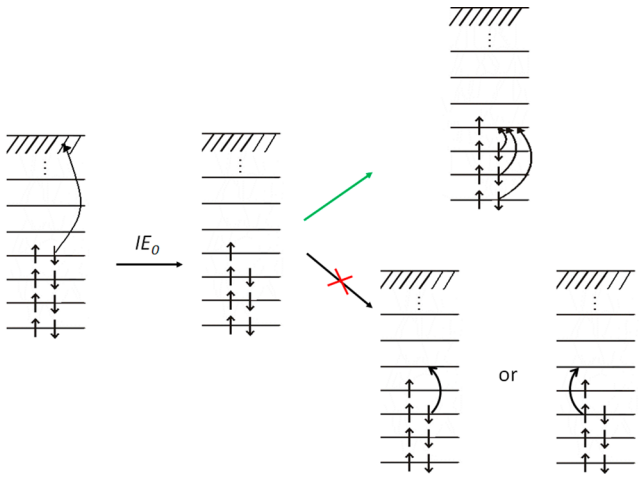

Figure 2. Calculation of ionization energies of tighter bound electrons by adding the excitation energies to SOMO within the ionized species to the lowest ionization energy. The green arrow points to the excitation in which SOMO is involved, while the red-crossed black arrow points to the excitation where SOMO is a spectator.

due to the poor description of dispersion interactions important, for example, for base pair stacking.[32] This issue is, however, of little relevance for the present work focusing on IEs of either individual DNA components or in the context of a piece of DNA the geometry of which is kept rigid. It would, however, be important for modeling of chemical rearrangements subsequent to photoionization of DNA.[33] In studies reported here, we use mostly the BMK functional with the aim of putting calculations of the lowest two IEs at the same methodological footing (vide infra). This in effect meant recalculating some of the IEs from our previous studies,[13,26,27] albeit with only minor changes of the actual values.

Higher IEs (i.e., those corresponding to the ionizations of the HOMO-1, etc., electrons) can be estimated from Koopmans theorem. While the theorem holds exactly for the HOMO within exact DFT, the orbital energies and ionization potentials differ significantly for commonly used approximate functionals. Recently, it has been shown that the DFT Koopmans theorem performs surprisingly well up to ∼30 eV IEs for the nonempirically tuned range separated density functionals.[34] It follows from Table 1 that orbital energies for these functionals indeed represent a very good approximation to ionization energies of the bases.

Another strategy to calculate higher ionization energies is to directly calculate energies of the parent species and the ground and excited states of the ionized species:

$$IE_{HOMO-n} = IE_{HOMO} + EE_n(ion)$$

where n is the index of the excited state and EE stands for excitation energy. The highly efficient TDDFT method employed here represents a pragmatic approach to achieve this goal even for large systems. The excited states of the ions could be in principle calculated more accurately, for example, using multireference methods[36,39] such as CASPT2 or using the SAC-CI method;[40] however, at orders of magnitude higher (and, therefore, prohibitive for larger systems) computational costs.

The TDDFT calculations should be executed with caution for systems with open shell reference. Excitations involving the singly occupied molecular orbital (SOMO) are typically described reliably within the TDDFT approach, with problems appearing in situations where SOMO acts as a spectator orbital.[41] From this point of view, it is good news that only excitations into the SOMO orbital are relevant for modeling ionization energies of an originally closed shell molecule (see Figure 2). Another potential problem connected with the TDDFT method is the appearance of spurious charge transfer states. These states can be efficiently eliminated by choosing hybrid functionals with a high content of exact exchange[42] or via long-range corrected (LC) functionals. Table 1 also demonstrates that under these circumstances the standard linear-response DFT/TDDFT approach works very well for low-lying ionization energies of nucleic acid bases. This highly efficient approach provides reliable results also for larger complexes, for example, IEs for a stacked thymine dimer are calculated 8.67 and 9.36 eV, compared to 8.78 and 9.30 eV calculated with the EOM-IP-CCSD/cc-pVTZ basis.[35]

Ionization of nucleic acid bases in the gas phase has been studied by post-Hartree−Fock methods such as MP2 or CCSD(T), multireference methods, EOM approaches or using strategies based on Green function formalism.[36,43,44] They all converge to similar values of IEs, which are, however, different from those encountered in fully solvated DNA. In particular, the EOM-CCSD-IP method[45] became frequently used in recent years to study ionization properties of DNA fragments.[30,46,47] For large systems, however, these methods become prohibitively expensive.

DOI: 10.1021/ar500366z
Acc. Chem. Res. 2015, 48, 1209−1217

4. INCLUDING SOLVENT EFFECTS: IS POLARIZABLE CONTINUUM GOOD ENOUGH?

A critical aspect underlying modeling of ionization of DNA and its components under biologically realistic conditions is a proper description of hydration. A new charged species is formed during ionization of a DNA base. Solvation energy of this nascent ion contributes significantly to the energetics of the ionization process. Starting with a rather crude Born model, the solvent correction to VIE of the neutral molecule is given as

$$\Delta \mathrm{VIE}_{\mathrm{solv}} = \frac{e^2}{8\pi\varepsilon_0 r}\left[1 - \frac{1}{\varepsilon_{\mathrm{opt}}}\right]$$

where r is the radius of the ion, e is elementary charge, and $\varepsilon_{\mathrm{opt}}$ is the optical (high-frequency) part of the dielectric constant. The optical part of dielectric constant appears in the formula since the nuclei are considered frozen during the vertical ionization process. In contrast, the solvent shift of the AIE, where full relaxation of the environment takes place, is due to both electronic and nuclear polarizations. The $\varepsilon_{\mathrm{opt}}$ has a value of around 2 for both aqueous and DNA environments, while the total dielectric constant of water is 80 and the total dielectric constant of the DNA environment was recently estimated to be around 8.[48] The screening effects of the electronic and nuclear polarization thus differ only by about a factor of 2 (note that the dielectric constant appears in the denominator in energy expressions). Indeed, the solvent shift is typically ~1 eV shift for the VIE and ~2 eV for the AIE for neutral solutes.[29] Also, based on the above considerations the interface between DNA and the aqueous solution is practically seamless with respect to effects on VIEs and even the effect on AIEs is minor (of the order of 0.1 eV).

Finally, the Born formula allows us to estimate the error introduced by simulations of the ionization in finite size systems. Asking for VIE accuracy of 0.2 eV, we need a water cavity with a diameter of about 1.8 nm which corresponds to about 200 water molecules. These semiquantitative considerations show that the often used microsolvation approach,[13,22,49−53] that is, gradual addition of a very small number of solvent molecules can hardly account for the very important bulk solvation effects.[13] Present day ab initio simulations typically allow for an explicit treatment of tens of solvent molecules within MD simulations which is, however, still not enough to fully converge the solvent effect. Such simulations can be accelerated by multilayer calculations, that is, within the ONIOM scheme or using QM/MM techniques. An interesting possibility used on several occasions in the context of nucleic acid ionization is employing the effective fragment potential (EFP) method, which takes into account electronic polarization and granularity of the solvent while keeping the computational expenses manageable.[54,55] Electronic polarization is, however, treated only within the linear response approximation.

The by far computationally most efficient way of including solvent effects is provided by dielectric continuum methods. There are various mutations of the dielectric continuum models; in our work we mostly rely on the polarizable continuum model (PCM) variant of the self consistent reaction field (SCRF).[56] The continuum approaches to solvation have been used in many applications.[48] Their use for the ionization process is, however, specific and needs to be done with care.[57,58] Only the electronic degrees of freedom (responsible for the optical part of the dielectric constant) should be allowed to relax during the VIE calculations, which is achieved via the nonequilibrium PCM (NEPCM) approach.[29,59−62] In contrast, the nuclear part of the dielectric response to ionization needs to be also included for the AIE calculations, e.g., when calculating the redox potentials or acidity constants.[63−68]

The dielectric models are developed within the linear response regime, ignoring the specific strong solvent−solute interactions. Therefore, they work reasonably well for neutral solutes. Applicability of the approach to ions is less well guaranteed as important specific effects connected, for example, with hydrogen bonds are missing.[69] By definition, we always encounter ions during the ionization process. This problem can be circumvented in the so-called cluster-continuum models,[13,26,31,70−72] which combine the microsolvation approach with dielectric continuum models. Nevertheless, it has been demonstrated recently that for DNA bases adding several explicit water molecules into the PCM cavity has only a minimal effect on the values of IEs.[73]

5. IONIZATION OF HYDRATED NUCLEIC ACID COMPONENTS

Individual gas phase or microhydrated nucleic acid components have been modeled extensively.[30,36,46,48,49,51−55,74−76] Their

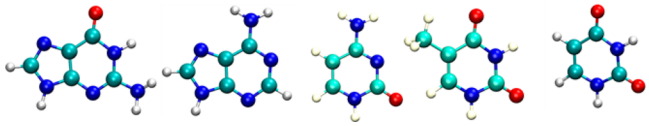

Figure 3. Structures of nucleic acid bases: from left to right guanine, adenine, cytosine, thymine, and uracil. We employ standard color coding, that is, carbon = cyan, nitrogen = blue, oxygen = red, and hydrogen = white.

Table 2. Lowest (first) and Second Lowest Vertical Ionization Energies (VIE) and Adiabatic Ionization Energy (AIE) of Nucleic Acid Bases in the Gas Phase and in the Aqueous Environment Calculated at the BMK/6-31+G* Level

	VIE				AIE	
base	first gas	second gas	first aq	second aq	gas	aq
G	8.08	9.64	7.29	9.18	7.68	5.84
A	8.34	9.32	7.59	8.77	8.10	6.21
C	8.78	9.39	8.03	8.58	8.66	6.64
T	9.09	10.09	8.05	9.37	8.82	6.60
U	9.55	10.19	8.42	9.43	9.29	6.93

Table 3. Ionization Characteristics for Nucleosides[a]

	VIE				AIE	
nucleoside	first gas	second gas	first aq	second aq	gas	aq
guanosine	7.86	9.44	7.26	8.96	7.41	5.85
adenosine	8.14	9.13	7.57	8.73	7.82	6.22
cytosine	8.46	9.17	7.84	8.49	7.98	6.54
deoxythymidine	8.56	9.66	7.81	9.06	8.27	6.46
uridine	8.96	9.84	8.19	9.21	8.69	6.82

[a]Conformations closest to the structural arrangement in the DNA are considered.

DOI: 10.1021/ar500366z
Acc. Chem. Res. 2015, 48, 1209−1217

Table 4. Ionization Characteristics for Nucleotides[a]

	VIE				AIE	
nucleotide	first gas	second gas	first aq	second aq	gas	aq
GMP^-	5.68	5.71	7.23	8.38	5.15	5.82
AMP^-	5.81	5.94	7.53	8.38	5.16	6.19
CMP^-	5.85	5.94	7.82	8.45	5.17	6.51
$deoxyTMP^-$	5.85	5.92	7.77	8.46	5.15	6.43
UMP^-	6.08	6.20	8.13	8.48	5.30	6.78

[a]Conformations closest to the structural arrangement in the DNA are considered.

modest size allows for application of high level electronic structure methods, with the price being only an indirect relation to biologically relevant aqueous environments.[27] Here, we employ the DFT/TDDFT framework, typically using the BMK functional[77] with the 6-31+G* basis set, together with the (NE)PCM model of the solvent,[56] yielding IEs with accuracy of ~0.2−0.3 eV. Such accuracy is sufficient for assigning and interpreting photoelectron spectra of aqueous DNA components.[26,27] Our most recent study, focused on determination of the related redox potentials by a combination of photoelectron spectroscopy and ab initio calculations, demonstrated the applicability of the present approach also for modeling primary redox processes.[78] This is also due to the fact that a significant part of our error is systematic (for the studied systems PCM tends to underestimate the solvent effects on IEs by 0.1−0.2 eV and the DFT method also has a comparably small systematic shift), which allows for higher accuracy in determining *relative* values when comparing different aqueous DNA components.[78] In addition, the present computational approach is highly efficient, allowing for screening of a large number of molecular systems.

The primary oxidation sites are the nucleic acid bases (Figure 3). Their calculated VIEs in the gas phase and in water represented by NEPCM are shown in Table 2. The purine bases, adenine and, in particular, guanine have lower ionization energies than the pyrimidine bases, cytosine, thymine, and uracil. The ordering remains the same in the aqueous phase, but the VIEs are all shifted down compared to the gas phase by about 1 eV. This shift is the effect of electronic polarization of the aqueous environment surrounding the bases. Nuclear relaxation pertinent to AIE adds further energy lowering of 1.2−1.4 eV. The effect of hydration on ionization energies is well captured within the PCM approach with additional microhydration changing the values by around 0.1−0.2 eV.[13] Test calculations for one of the bases, uracil, also show that employing another widely used continuum solvation model (SMD)[79] leads only to minor changes of the two lowest VIEs, yielding 8.23 and 9.48 eV (compare to last line in Table 2). This is in line with a recent comparison of several continuum solvation models.[80] Unlike in the gas phase, tautomerism does not play an important role for the ionization of the bases in water as only one or two tautomers are populated at ambient conditions.

Direct comparison of the calculated IEs with the PE experiments is impaired by the low solubility of the isolated bases.[78] Nevertheless, the VIEs can be compared for the more soluble nucleosides (see Table 3), demonstrating a very good performance of the present computational approach.[26,78] The effect of the sugar on the VIE is negligible for purine nucleosides due to large separation of orbital energies between the sugar and the base. The sugar has a slightly larger effect for the pyrimidines in the gas phase. In water, the effect of adding ribose or deoxyribose on the VIE is, however, always smaller than 0.2 eV (Tables 2 and 3).

The phosphate anion in nucleotides represents a potentially significant perturbation of the electronic structure of the system (see Tables 4 and 5). First, the extra electron of the anion is typically weakly bound. On top of that, the negative charge of the anion destabilizes the neighboring electrons on the base leading to decrease of VIE in the gas phase by more than 2 eV. Both effects are, however, suppressed in water, where lowest ionization takes place from the base and the VIEs are almost the same as for the nucleosides.

Let us discuss in more detail the stabilization effect of water for isolated phosphate anions (see Table 5 and Figure 4). Monovalent $H_2PO_4^-$ anion is electronically stable already in the gas phase with a calculated VIE around 5 eV, close to the experimental value of 5.06 eV.[81] In water, the calculated VIE shifts to about 9 eV due to a strong solvent stabilization of the anion. The dielectric continuum model is acceptable but not fully quantiative for the monovalent anion as documented by Figure 4 (right), which shows the VIE convergence with number of explicit water molecules. The limiting value of 9.65 eV for 64 explicit water molecules embedded in a dielectric continuum is already in a good agreement with the experiment. The solvent effect is even more pronounced for the doubly charged HPO_4^{2-} anion which is not stable in the gas phase and for which the convergence in VIE with the number of explicit water molecules embedded in a dielectric continuum is slower (Figure 4, left). Note that while the protonation state has a sizable influence on the value of the VIE of the aqueous phosphate ion, the effect of counterions is much smaller.[31] Finally, within the context of DNA components, we have shown recently that adding explicit water molecules into the PCM cavity has only a minor effect on the lowest ionization energy (with ionization originating from the base) of singly and even doubly charged nucleotides.[82]

6. IONIZATION OF DNA: A BOTTOM-UP APPROACH

Nucleic acid bases within the native DNA specifically interact via hydrogen bonds and stacking interactions with neighboring bases or electrostatically with the charged backbone, water, and

Table 5. Ionization Characteristics of the Remaining Nucleic Acid Components

	VIE				AIE	
others	first gas	second gas	first aq	second aq	gas	aq
ribose	9.62	9.83	8.61	9.83	8.96	7.00
deoxyribose	9.52	10.21	8.59	10.21	8.80	6.76
HPO4[2]	5.13	5.25	8.79/9.65[a]	8.90	4.33	7.88
HPO_4^{2-}	unstable	unstable	6.91/9.0[a]	7.35	unstable	5.25

[a]Hybrid explicit solvent/NEPCM model.

DOI: 10.1021/ar500366z
Acc. Chem. Res. 2015, 48, 1209−1217

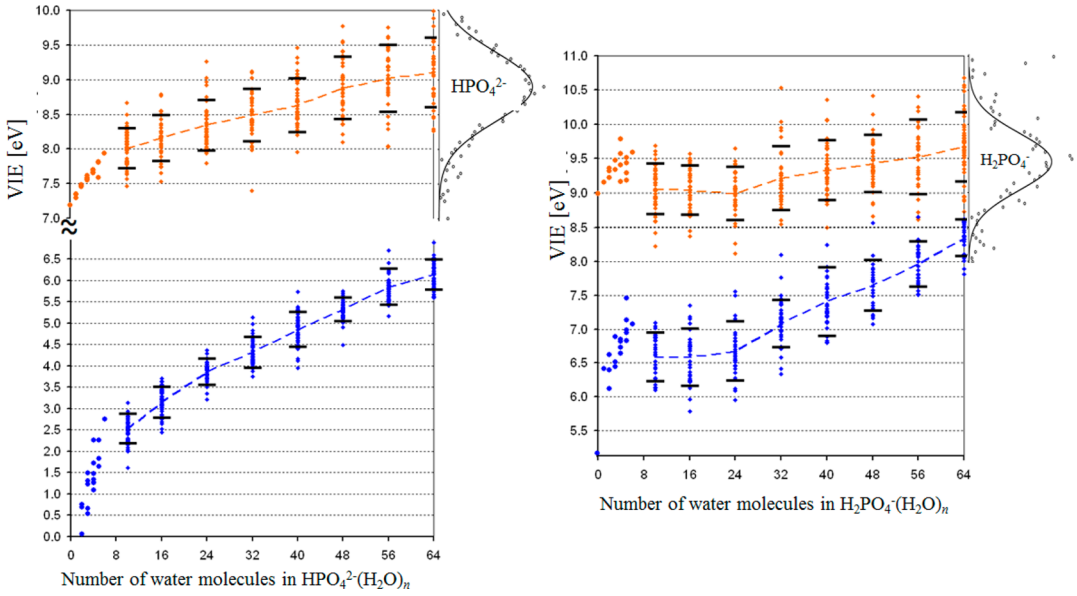

Figure 4. Lowest vertical ionization energy of $HPO_4^{2-}(H_2O)_{0-64}$ (left) and $H_2PO_4^{-}(H_2O)_{0-64}$ (right) in the gas phase (blue symbols) or in solution modeled via a hybrid explicit solvent/NEPCM approach (orange symbols). Adapted with permission from ref 31. Copyright 2012 American Chemical Society.

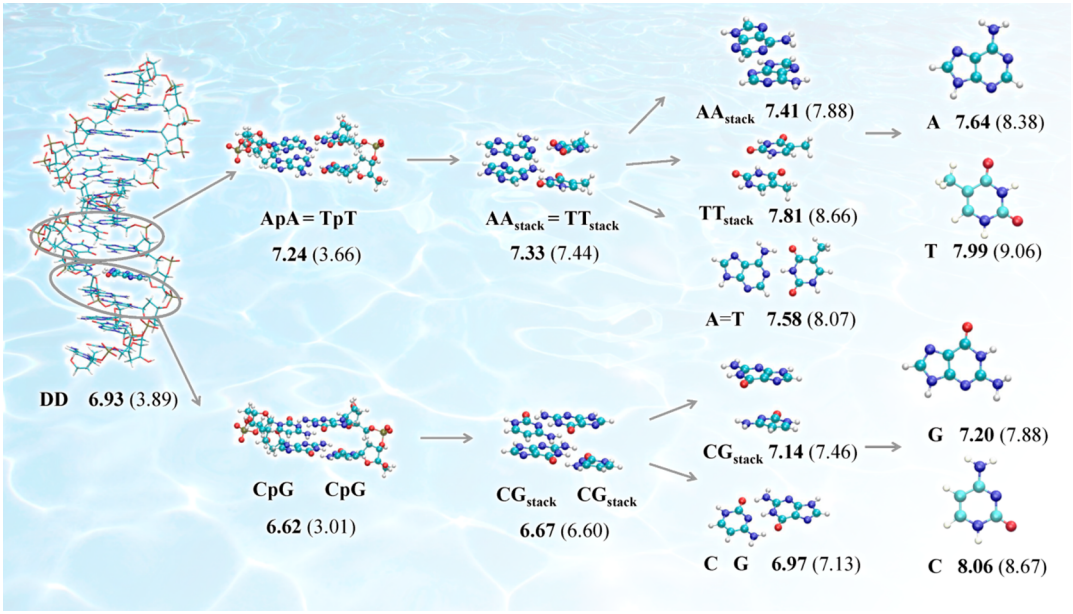

Figure 5. Vertical ionization energies (in eV) of the Dickerson dodecamer and its fragments. The aqueous environment is modeled by PCM, with the gas phase VIE values presented in parentheses. The VIE of the whole dodecamer (neutralized by sodium cations) was estimated by polarizable embedding[27] of guanine (at the BMK/6-31+G* level) into DD (at the PM6 level). The upper row shows fragmentation of DD to hydrogen bonded thymine dinucleotide and an adenine dinucleotide (TpT = ApA), hydrogen bonded AA and TT stacks ($TT_{stack} = AA_{stack}$), AA_{stack} and TT_{stack} and A = T base pair, and finally to adenine and thymine bases. The lower row show analogous fragmentation to hydrogen bonded cytosine-guanine dinucleotides (CpG ≡ CpG), two hydrogen bonded CG stacks ($CG_{stack} \equiv CG_{stack}$), CG_{stack} stack and C ≡ G base pair, and finally to guanine and cytosine bases. The fragments were capped with hydrogen atoms if needed. No further optimization was performed.

the counterions. Such a highly organized environment could in principle lead to significant changes in the ionization characteristics compared to individual aqueous bases,[83] however, it turns out that the effect is rather modest.[27] This is demonstrated here on a fully hydrated (with counterions) piece of DNA, the so-called Dickerson dodecamer (DD),[84] and its fragments. The corresponding VIEs are presented in Figure 5. Note that the long-range solvent polarization has a dominating role on calculated VIEs.

Let us now follow the gradual turning on of the specific interactions for the guanine molecule (Figure 5). Aqueous guanine has the lowest VIE among the bases of 7.2 eV. This value is shifted down by 0.2 eV upon hydrogen bonding with cytosine. The stacking with cytosine has only a negligible effect on the VIE since the electronic resonance with a unit of significantly higher VIE is negligible. There is, nevertheless, a drop of 0.3 eV in the VIE for the $CG_{stack} \equiv CG_{stack}$ tetramer. This is mostly due to electronic interactions between the two

DOI: 10.1021/ar500366z
Acc. Chem. Res. 2015, 48, 1209−1217

guanine units. Such effect can be described neither by the dielectric environment, nor within the QM/MM or QM/QM schemes. The minimum DNA model to be used, for example, in modeling the transport processes or sequence specific effects should thus contain at least two stacks of hydrogen bonded bases in a single QM region. The dielectric continuum solvent, nevertheless, safely screens the sugar−phosphate backbone with the counterions.

7. CONCLUSIONS

The emerging photoelectron experiments in microjets provide hitherto unavailable benchmarks for theoretical calculations of ionization energies in aqueous solutions. These measurements yield, however, only fragmentary data; therefore, theoretical modeling is imperative for full mechanistic understanding of DNA ionization and subsequent hole or electron transfer. Based on comparison to aqueous photoelectron spectroscopy and benchmark calculations we argue that carefully chosen variants of density functional theory can be used for accurate modeling of ionization spectra and primary redox properties (before subsequent deprotonation reactions and thus hardly accessible to standard electrochemical methods) of DNA components within the native environment of the double helix. It is however imperative to account for long-range polarization effects of the aqueous solvent, which is achieved within the dielectric continuum models.

The present results demonstrate that specific interactions between the subunits of DNA are efficiently screened by the aqueous solvent and, consequently, the ionization characteristics can be modeled by focusing on individual aqueous fragments (i.e., bases, nucleosides, or nucleotides). The remarkable screening ability of the aqueous solvent thus facilitates modeling of ionization in this highly complex biomolecular system employing an additive approach. The residual nonadditivity stems from electronic interaction between adjacent base pairs, which should be accounted for most accurate modeling.

In summary, we present here a robust and computationally efficient quantum chemical methodology for calculating vertical and adiabatic ionization energies of DNA and its components in the native aqueous environment. Vertical ionization energies directly correlate with peaks in photoelectron spectra in liquid microjets,[26,27] while the adiabatic ionization energies can be related to threshold ionization values of aqueous DNA interesting also from the point of view of the possibility of DNA ionization by the UV edge of the solar spectrum.[85,86] Moreover, reorganization energies, calculated as differences between VIEs and AIEs, can be combined with results from photoelectron spectroscopy[78] to provide accurate estimates of redox potentials corresponding to primary redox processes in DNA.

AUTHOR INFORMATION

Corresponding Authors

*E-mail: petr.slavicek@vscht.cz (P.S.).
*E-mail: pavel.jungwirth@uochb.cas.cz (P.J.).

Present Address

§E.P.: Department of Chemistry, École Normale Supérieure, UMR ENS-CNRS-UPMC 8640, 24 rue Lhomond, 75005 Paris, France.

Notes

The authors declare no competing financial interest.

Biographies

Eva Pluhařová (*1986) is currently a postdoc at École Normale Supérieure in Paris in the group of Damien Laage. During her graduate and undergraduate studies with Pavel Jungwirth and Petr Slavíček, she focused on solvent effect on ion pairing and photoionization in water. She obtained her Ph.D. degree at the Charles University in Prague in 2014.

Petr Slavíček (*1976) is a professor of physical chemistry at the University of Chemistry and Technology, Prague and research associate at the Jaroslav Heyrovský Institute of Physical Chemistry of the Academy of Sciences of the Czech Republic. He obtained his Ph.D. degree at the Charles University in Prague and spent then 2 years as a postdoc in the group of Todd Martínez at the University of Illinois. In his work, he focuses on simulations of light induced processes in solvated systems.

Pavel Jungwirth (*1966) is a senior research group head at the Institute of Organic Chemistry and Biochemistry of the Academy of Sciences of the Czech Republic and full professor in physics at the Charles University in Prague. He got involved with DNA ionization and solvated electrons during a short sabbatical with his experimental colleague and friend Steve Bradforth at USC in Los Angeles in 2007. This has been so much fun that it almost grew out of control; nevertheless, his core scientific interests involve modeling of ion−protein interactions (Hofmeister series) and processes in cellular membranes.

ACKNOWLEDGMENTS

We thank our experimental colleagues Steve Bradforth and Bernd Winter for wonderful collaboration and valuable discussions. P.J. thanks the Czech Science Foundation (Grant P208/12/G016) and the Academy of Sciences (Praemium Academie Award). P.S. thanks the Czech Science Foundation (Grant 13-34168S). E.P. thanks the International Max-Planck Research School for support.

REFERENCES

(1) Lehnert, S. *Biomolecular Action of Ionizing Radiation*; CRC Press: Boca Raton, FL, 2007.
(2) Morgan, W. F. Non-targeted and Delayed Effects of Exposure to Ionizing Radiation: II. Radiation-induced Genomic Instability and Bystander Effects in vivo, Clastogenic Factors and Transgenerational Effects. *Radiat. Res.* **2003**, *159*, 581−596.
(3) Genereux, J. C.; Boal, A. K.; Barton, J. K. DNA-Mediated Charge Transport in Redox Sensing and Signaling. *J. Am. Chem. Soc.* **2010**, *132*, 891−905.
(4) Giese, B. Long-distance Electron Transfer Through DNA. *Annu. Rev. Biochem.* **2002**, *71*, 51−70.
(5) Kawai, K.; Majima, T. Hole Transfer Kinetics of DNA. *Acc. Chem. Res.* **2013**, *46*, 2616−2625.
(6) Saito, I.; Takayama, M.; Sugiyama, H.; Nakatani, K. Photo-induced DNA Cleavage Via Electron-transfer - Demonstration That Guanine Residues Located 5′ To Guanine are the most Electron-donating Sites. *J. Am. Chem. Soc.* **1995**, *117*, 6406−6407.
(7) Retel, J.; Hoebee, B.; Braun, J. E. F.; Lutgerink, J. T.; Vandenakker, E.; Wanamarta, A. H.; Joenje, H.; Lafleur, M. V. M Mutational Specificity of Oxidative DNA Damage. *Mutat. Res.* **1993**, *299*, 165−182.
(8) Jovanovic, S. V.; Simic, M. G. One-electron Redox Potentials of Purines and Pyrimidines. *J. Phys. Chem.* **1986**, *90*, 974−978.

DOI: 10.1021/ar500366z
Acc. Chem. Res. 2015, 48, 1209−1217

(9) Steenken, S.; Jovanovic, S. V. How Easily Oxidizable is DNA? One-electron Reduction Potentials of Adenosine and Guanosine Radicals in Aqueous Solution. *J. Am. Chem. Soc.* **1997**, *119*, 617−618.
(10) Steenken, S.; Telo, J. P.; Novais, H. M.; Candeias, L. P. One-Electron-Reduction Potentials of Pyrimidine-Bases, Nucleosides, and Nucleotides in Aqueous-Solution - Consequences for DNA Redox Chemistry. *J. Am. Chem. Soc.* **1992**, *114*, 4701−4709.
(11) Siriwong, K.; Voityuk, A. A. Electron Transfer in DNA. *Wiley Interdiscip. Rev.: Comput. Mol. Sci.* **2012**, *2*, 780−794.
(12) Siriwong, K.; Voityuk, A. A.; Berlin, Y. A. Can Charge Recombination in DNA Hairpins Be Controlled by Counterions? *J. Phys. Chem. C* **2010**, *114*, 20503−20509.
(13) Pluharova, E.; Jungwirth, P.; Bradforth, S. E.; Slavicek, P. Ionization of Purine Tautomers in Nucleobases, Nucleosides, and Nucleotides: From the Gas Phase to the Aqueous Environment. *J. Phys. Chem. B* **2011**, *115*, 1294−1305.
(14) Chatterley, A. S.; Johns, A. S.; Stavros, V. G.; Verlet, J. R. R. Base-Specific Ionization of Deprotonated Nucleotides by Resonance Enhanced Two-Photon Detachment. *J. Phys. Chem. A* **2013**, *117*, 5299−5305.
(15) Chatterley, A. S.; West, C. W.; Roberts, G. M.; Stavros, V. G.; Verlet, J. R. R. Mapping the Ultrafast Dynamics of Adenine onto Its Nucleotide and Oligonucleotides by Time-Resolved Photoelectron Imaging. *J. Phys. Chem. Lett.* **2014**, *5*, 843−848.
(16) Yang, X.; Wang, X. B.; Vorpagel, E. R.; Wang, L. S. Direct Experimental Observation of the Low Ionization Potentials of Guanine in Free Oligonucleotides by Using Photoelectron Spectroscopy. *Proc. Natl. Acad. Sci. U. S. A.* **2004**, *101*, 17588−17592.
(17) Belau, L.; Wilson, K. R.; Leone, S. R.; Ahmed, M. Vacuum-ultraviolet Photoionization Studies of the Microhydration of DNA Bases (Guanine, Cytosine, Adenine, and Thymine). *J. Phys. Chem. A* **2007**, *111*, 7562−7568.
(18) Stokes, S. T.; Grubisic, A.; Li, X.; Ko, Y. J.; Bowen, K. H. Photoelectron Spectroscopy of the Parent Anions of the Nucleotides, Adenosine-5′-Monophosphate and 2′-Deoxyadenosine-5′-Monophosphate. *J. Chem. Phys.* **2008**, *128*, 044314.
(19) Crespo-Hernandez, C. E.; Arce, R. Photoionization of DNA and RNA Bases, Nucleosides and Nucleotides Through a Combination of One- and Two-photon Pathways upon 266 nm Nanosecond Laser Excitation. *Photochem. Photobiol.* **2002**, *76*, 259−267.
(20) Kim, H. S.; Yu, M.; Jiang, Q.; Lebreton, P. R. UB Photoelectron and Ab-Initio Quantum-Mechanical Characterization of 2′-Deoxyguanosine 5′-Phosphate - Electronic Influences on DNA Alkylation Patterns. *J. Am. Chem. Soc.* **1993**, *115*, 6169−6183.
(21) Orlov, V. M.; Smirnov, A. N.; Varshavsky, Y. M. Ionization-Potentials and Electron-Donor Ability of Nucleic-Acid Bases and Their Analogs. *Tetrahedron Lett.* **1976**, *17*, 4377−4378.
(22) Ghosh, D.; Golan, A.; Takahashi, L. K.; Krylov, A. I.; Ahmed, M. A VUV Photoionization and Ab Initio Determination of the Ionization Energy of a Gas-Phase Sugar (Deoxyribose). *J. Phys. Chem. Lett.* **2012**, *3*, 97−101.
(23) Fernando, H.; Papadantonakis, G. A.; Kim, N. S.; LeBreton, P. R. Conduction-Band-Edge Ionization thresholds of DNA Components in Aqueous Solution. *Proc. Natl. Acad. Sci. U. S. A.* **1998**, *95*, 5550−5555.
(24) Seidel, R.; Thurmer, S.; Winter, B. Photoelectron Spectroscopy Meets Aqueous Solution: Studies from a Vacuum Liquid Microjet. *J. Phys. Chem. Lett.* **2011**, *2*, 633−641.
(25) Winter, B.; Faubel, M. Photoemission from Liquid Aqueous Solutions. *Chem. Rev.* **2006**, *106*, 1176−1211.
(26) Slavicek, P.; Winter, B.; Faubel, M.; Bradforth, S. E.; Jungwirth, P. Ionization Energies of Aqueous Nucleic Acids: Photoelectron Spectroscopy of Pyrimidine Nucleosides and ab Initio Calculations. *J. Am. Chem. Soc.* **2009**, *131*, 6460−6467.
(27) Pluharova, E.; Schroeder, C.; Seidel, R.; Bradforth, S. E.; Winter, B.; Faubel, M.; Slavicek, P.; Jungwirth, P. Unexpectedly Small Effect of the DNA Environment on Vertical Ionization Energies of Aqueous Nucleobases. *J. Phys. Chem. Lett.* **2013**, *4*, 3766−3769.
(28) Koch, W.; Holthausen, M. C. *A Chemist's Guide to Density Functional Theory*; Wiley-VCH: Weinheim, 2000.
(29) Jagoda-Cwiklik, B.; Slavicek, P.; Cwiklik, L.; Nolting, D.; Winter, B.; Jungwirth, P. Ionization of Imidazole in the Gas Phase, Microhydrated Environments, and in Aqueous Solution. *J. Phys. Chem. A* **2008**, *112*, 3499−3505.
(30) Bravaya, K. B.; Epifanovsky, E.; Krylov, A. I. Four Bases Score a Run: Ab Initio Calculations Quantify a Cooperative Effect of H-Bonding and pi-Stacking on the Ionization Energy of Adenine in the AATT Tetramer. *J. Phys. Chem. Lett.* **2012**, *3*, 2726−2732.
(31) Pluharova, E.; Oncak, M.; Seidel, R.; Schroeder, C.; Schroeder, W.; Winter, B.; Bradforth, S. E.; Jungwirth, P.; Slavicek, P. Transforming Anion Instability into Stability: Contrasting Photoionization of Three Protonation Forms of the Phosphate Ion upon Moving into Water. *J. Phys. Chem. B* **2012**, *116*, 13254−13264.
(32) Zhao, Y.; Truhlar, D. G. Density Functionals with Broad Applicability in Chemistry. *Acc. Chem. Res.* **2008**, *41*, 157−167.
(33) Khanduri, D.; Adhikary, A.; Sevilla, M. D. Highly Oxidizing Excited States of One-Electron-Oxidized Guanine in DNA: Wavelength and pH Dependence. *J. Am. Chem. Soc.* **2011**, *133*, 4527−4537.
(34) Baer, R.; Livshits, E.; Salzner, U. Tuned Range-Separated Hybrids in Density Functional Theory. *Annu. Rev. Phys. Chem.* **2010**, *61*, 85−109.
(35) Bravaya, K. B.; Kostko, O.; Ahmed, M.; Krylov, A. I. The effect of Pi-stacking, H-bonding, and Electrostatic Interactions on the Ionization Energies of Nucleic Acid Bases: Adenine-Adenine, Thymine-Thymine and Adenine-Thymine Dimers. *Phys. Chem. Chem. Phys.* **2010**, *12*, 2292−2307.
(36) Roca-Sanjuan, D.; Rubio, M.; Merchan, M.; Serrano-Andres, L. Ab initio Determination of the Ionization Potentials of DNA and RNA Nucleobases. *J. Chem. Phys.* **2006**, *125*, 084302.
(37) Faber, C.; Attaccalite, C.; Olevano, V.; Runge, E.; Blase, X. First-Principles GW Calculations for DNA and RNA Nucleobases. *Phys. Rev. B* **2011**, *83*, 115123.
(38) Hush, N. S.; Cheung, A. S. Ionization-Potentials and Donor Properties of Nucleic-Acid Bases and Related Compounds. *Chem. Phys. Lett.* **1975**, *34*, 11−13.
(39) Roca-Sanjuan, D.; Merchan, M.; Serrano-Andres, L. Modeling Hole Transfer in DNA: Low-lying Excited States of Oxidized Cytosine Homodimer and Cytosine-Adenine Heterodimer. *Chem. Phys.* **2008**, *349*, 188−196.
(40) Farrokhpour, H.; Ghandehari, M. Photoelectron Spectra of Some Important Biological Molecules: Symmetry-Adapted-Cluster Configuration Interaction Study. *J. Phys. Chem. B* **2013**, *117*, 6027−6041.
(41) Ipatov, A.; Cordova, F.; Doriol, L. J.; Casida, M. E. Excited-State Spin-Contamination in Time-Dependent Density-Functional Theory for Molecules with Open-Shell Ground States. *J. Mol. Struct.: THEOCHEM* **2009**, *914*, 60−73.
(42) Magyar, R. J.; Tretiak, S. Dependence of Spurious Charge-Transfer Excited States on Orbital Exchange in TDDFT: Large Molecules and Clusters. *J. Chem. Theory Comput.* **2007**, *3*, 976−987.
(43) Zakjevskii, V. V.; King, S. J.; Dolgounitcheva, O.; Zakrzewski, V. G.; Ortiz, J. V. Base and Phosphate Electron Detachment Energies of Deoxyribonucleotide Anions. *J. Am. Chem. Soc.* **2006**, *128*, 13350−13351.
(44) Cauet, E.; Dehareng, D.; Lievin, J. Ab initio Study of the Ionization of the DNA Bases: Ionization Potentials and Excited States of the Cations. *J. Phys. Chem. A* **2006**, *110*, 9200−9211.
(45) Stanton, J. F.; Gauss, J. Analytic Energy Derivatives for Ionized States Described by the Equation-of-Motion Coupled-Cluster Method. *J. Chem. Phys.* **1994**, *101*, 8938−8944.
(46) Bravaya, K. B.; Kostko, O.; Dolgikh, S.; Landau, A.; Ahmed, M.; Krylov, A. I. Electronic Structure and Spectroscopy of Nucleic Acid Bases: Ionization Energies, Ionization-Induced Structural Changes, and Photoelectron Spectra. *J. Phys. Chem. A* **2010**, *114*, 12305−12317.
(47) Zadorozhnaya, A. A.; Krylov, A. I. Zooming into pi-Stacked Manifolds of Nucleobases: Ionized States of Dimethylated Uracil Dimers. *J. Phys. Chem. A* **2010**, *114*, 2001−2009.

DOI: 10.1021/ar500366z
Acc. Chem. Res. 2015, 48, 1209−1217

(48) Cuervo, A.; Dans, P. D.; Carrascosa, J. L.; Orozco, M.; Gomila, G.; Fumagalli, L. Direct Measurement of the Dielectric Polarization Properties of DNA. *Proc. Natl. Acad. Sci. U. S. A.* **2014**, *111*, E3624−E3630.
(49) Close, D. M.; Crespo-Hernandez, C. E.; Gorb, L.; Leszczynski, J. The Influence of Microhydration on the Ionization Energy Thresholds of Uracil and Thymine. *J. Phys. Chem. A* **2005**, *109*, 9279−9283.
(50) Close, D. M.; Crespo-Hernandez, C. E.; Gorb, L.; Leszczynski, J. Theoretical Elucidation of Conflicting Experimental Data on Vertical Ionization Potentials of Microhydrated Thymine. *J. Phys. Chem. A* **2008**, *112*, 4405−4409.
(51) Close, D. M.; Crespo-Hernandez, C. E.; Gorb, L.; Leszczynski, J. Ionization Energy Thresholds of Microhydrated Adenine and Its Tautomers. *J. Phys. Chem. A* **2008**, *112*, 12702−12706.
(52) Colson, A. O.; Besler, B.; Sevilla, M. D. Ab-Initio Molecular-Orbital Calculations an DNA Radical Ions 0.4. Effect of Hydration an Electron-Affinities and Ionization-Potentials of Base-Pairs. *J. Phys. Chem.* **1993**, *97*, 13852−13859.
(53) Khistyaev, K.; Bravaya, K. B.; Kamarchik, E.; Kostko, O.; Ahmed, M.; Krylov, A. I. The Effect of Microhydration on Ionization Energies of Thymine. *Faraday Discuss.* **2011**, *150*, 313−330.
(54) Ghosh, D.; Isayev, O.; Slipchenko, L. V.; Krylov, A. I. Effect of Solvation on the Vertical Ionization Energy of Thymine: From Microhydration to Bulk. *J. Phys. Chem. A* **2011**, *115*, 6028−6038.
(55) Ghosh, D.; Roy, A.; Seidel, R.; Winter, B.; Bradforth, S.; Krylov, A. I. First-Principle Protocol for Calculating Ionization Energies and Redox Potentials of Solvated Molecules and Ions: Theory and Application to Aqueous Phenol and Phenolate. *J. Phys. Chem. B* **2012**, *116*, 7269−7280.
(56) Tomasi, J.; Mennucci, B.; Cammi, R. Quantum Mechanical Continuum Solvation Models. *Chem. Rev.* **2005**, *105*, 2999−3093.
(57) Close, D. M. Calculation of the Ionization Potentials of the DNA Bases in Aqueous Medium. *J. Phys. Chem. A* **2004**, *108*, 10376−10379.
(58) Crespo-Hernandez, C. E.; Arce, R.; Ishikawa, Y.; Gorb, L.; Leszczynski, J.; Close, D. M. Ab Initio Ionization Energy Thresholds of DNA and RNA Bases in Gas Phase and in Aqueous Solution. *J. Phys. Chem. A* **2004**, *108*, 6373−6377.
(59) Mennucci, B.; Cammi, R.; Tomasi, J. Excited States and Solvatochromic Shifts within a Nonequilibrium Solvation Approach: A new Formulation of the Integral Equation Formalism Method at the Self-Consistent Field, Configuration Interaction, and Multiconfiguration Self-Consistent Field level. *J. Chem. Phys.* **1998**, *109*, 2798−2807.
(60) Jagoda-Cwiklik, B.; Slavicek, P.; Nolting, D.; Winter, B.; Jungwirth, P. Ionization of Aqueous Cations: Photoelectron Spectroscopy and Ab Initio Calculations of Protonated Imidazole. *J. Phys. Chem. B* **2008**, *112*, 7355−7358.
(61) Cossi, M.; Barone, V. Separation Between Fast and Slow Polarizations in Continuum Solvation Models. *J. Phys. Chem. A* **2000**, *104*, 10614−10622.
(62) Sistik, L.; Oncak, M.; Slavicek, P. Simulations of Photoemission and Equilibrium Redox Processes of Ionic Liquids: The Role of Ion Pairing and Long-Range Polarization. *Phys. Chem. Chem. Phys.* **2011**, *13*, 11998−12007.
(63) Psciuk, B. T.; Lord, R. L.; Munk, B. H.; Schlegel, H. B. Theoretical Determination of One-Electron Oxidation Potentials for Nucleic Acid Bases. *J. Chem. Theory Comput.* **2012**, *8*, 5107−5123.
(64) Crespo-Hernandez, C. E.; Close, D. M.; Gorb, L.; Leszczynski, J. Determination of Redox Potentials for the Watson-Crick Base Pairs, DNA Nucleosides, and Relevant Nucleoside Analogues. *J. Phys. Chem. B* **2007**, *111*, 5386−5395.
(65) Paukku, Y.; Hill, G. Theoretical Determination of One-Electron Redox Potentials for DNA Bases, Base Pairs, and Stacks. *J. Phys. Chem. A* **2011**, *115*, 4804−4810.
(66) Marenich, A. V.; Ho, J.; Coote, M. L.; Cramer, C. J.; Truhlar, D. G. Computational electrochemistry: prediction of liquid-phase reduction potentials. *Phys. Chem. Chem. Phys.* **2014**, *16*, 15068−15106.
(67) Ho, J.; Coote, M. L. First-principles prediction of acidities in the gas and solution phase. *Wiley Interdiscip. Rev.: Comput. Mol. Sci.* **2011**, *1*, 649−660.
(68) Ho, J. Are thermodynamic cycles necessary for continuum solvent calculation of pK(a)s and reduction potentials? *Phys. Chem. Chem. Phys.* **2015**, *17*, 2859−2868.
(69) Cramer, C. J.; Truhlar, D. G. A Universal Approach to Solvation Modeling. *Acc. Chem. Res.* **2008**, *41*, 760−768.
(70) Thapa, B.; Schlegel, H. B. Calculations of pK_a's and Redox Potentials of Nucleobases with Explicit Waters and Polarizable Continuum Solvation. *J. Phys. Chem. A* **2014**, DOI: 10.1021/jp5088866.
(71) Zakjevskii, V. V.; King, S. J.; Dolgounitcheva, O.; Zakrzewski, V. G.; Ortiz, J. V. Base and Phosphate Electron Detachment Energies of Deoxyribonucleotide Anions. *J. Am. Chem. Soc.* **2006**, *128*, 13350−13351.
(72) Dolgounitcheva, O.; Zakrzewski, V. G.; Ortiz, J. V. Ionization Energies and Dyson Orbitals of Cytosine and 1-Methylcytosine. *J. Phys. Chem. A* **2003**, *107*, 822−828.
(73) Pliego, J. R.; Riveros, J. M. Theoretical calculation of pK_a using the cluster-continuum model. *J. Phys. Chem. A* **2002**, *106*, 7434−7439.
(74) Kelly, C. P.; Cramer, C. J.; Truhlar, D. G. Adding explicit solvent molecules to continuum solvent calculations for the calculation of aqueous acid dissociation constants. *J. Phys. Chem. A* **2006**, *110*, 2493−2499.
(75) Ho, J.; Coote, M. L. A universal approach for continuum solvent pK_a calculations: Are we there yet? *Theor. Chem. Acc.* **2010**, *125*, 3−21.
(76) Singh, R. K.; Ortiz, J. V.; Mishra, M. K. Tautomeric Forms of Adenine: Vertical Ionization Energies and Dyson Orbitals. *Int. J. Quantum Chem.* **2010**, *110*, 1901−1915.
(77) Boese, A. D.; Martin, J. M. L. Development of Density Functionals for Thermochemical Kinetics. *J. Chem. Phys.* **2004**, *121*, 3405−3416.
(78) Schroeder, C. A.; Pluharova, E.; Seidel, R.; Schroder, W. P.; M, F.; Slavicek, P.; Winter, B.; Jungwirth, P.; Bradforth, S. E. Oxidation Half-Reaction of Aqueous Nucleosides and Nucleotides via Photoelectron Spectroscopy Augmented by Ab Initio Calculations. *J. Am. Chem. Soc.* **2015**, *137*, 201−209.
(79) Marenich, A. V.; Cramer, C. J.; Truhlar, D. G. Universal Solvation Model Based on Solute Electron Density and on a Continuum Model of the Solvent Defined by the Bulk Dielectric Constant and Atomic Surface Tensions. *J. Phys. Chem. B* **2009**, *113*, 6378−6396.
(80) Klamt, A.; Mennucci, B.; Tomasi, J.; Barone, V.; Curutchet, C.; Orozco, M.; Luque, F. J. On the Performance of Continuum Solvation Methods. A Comment on "Universal Approaches to Solvation Modeling". *Acc. Chem. Res.* **2009**, *42*, 489−492.
(81) Wang, X. B.; Vorpagel, E. R.; Yang, X.; Wang, L. S. Experimental and Theoretical Investigations of the Stability, Energetics, and Structures, of $H_2PO_4^-$, $H_2P_2O_7^{2-}$, and $H_3P_3O_{10}^{2-}$ in the gas phase. *J. Phys. Chem. A* **2001**, *105*, 10468−10474.
(82) Palivec, V.; Pluharova, E.; Unger, I.; Winter, B.; Jungwirth, P. DNA Lesion Can Facilitate Base Ionization: Vertical Ionization Energies of Aqueous 8-Oxoguanine and its Nucleoside and Nucleotide. *J. Phys. Chem. B* **2014**, *118*, 13833−13837.
(83) Cauet, E.; Valiev, M.; Weare, J. H. Vertical Ionization Potentials of Nucleobases in a Fully Solvated DNA Environment. *J. Phys. Chem. B* **2010**, *114*, 5886−5894.
(84) Tjandra, N.; Tate, S.; Ono, A.; Kainosho, M.; Bax, A. The NMR Structure of a DNA Dodecamer in an Aqueous Dilute Liquid Crystalline Phase. *J. Am. Chem. Soc.* **2000**, *122*, 6190−6200.
(85) Papadantonakis, G. A.; Tranter, R.; Brezinsky, K.; Yang, Y. N.; van Breemen, R. B.; LeBreton, P. R. Low-Energy, Low-Yield Photoionization, and Production of 8-Oxo-2′-deoxyguanosine and Guanine from 2′-Deoxyguanosine. *J. Phys. Chem. B* **2002**, *106*, 7704−7712.
(86) Crespo-Hernandez, C. E.; Cohen, B.; Hare, P. M.; Kohler, B. Ultrafast Excited-State Dynamics in Nucleic Acids. *Chem. Rev.* **2004**, *104*, 1977−2020.

DOI: 10.1021/ar500366z
Acc. Chem. Res. 2015, 48, 1209−1217